IOP FTC
IOP PUBLISHING JOURNAL OF PHYSICS A: MATHEMATICAL AND THEORETICAL

J. Phys. A: Math. Theor. **41** (2008) 252001 (7pp) doi:10.1088/1751-8113/41/25/252001

FAST TRACK COMMUNICATION

Hierarchical regular small-world networks

Stefan Boettcher[1], **Bruno Gonçalves**[1] **and Hasan Guclu**[2]

[1] Department of Physics, Emory University, Atlanta, GA 30322, USA
[2] Center for Nonlinear Studies, Los Alamos National Laboratory, MS-B258, Los Alamos, NM 87545, USA

Received 31 March 2008, in final form 1 April 2008
Published 27 May 2008
Online at stacks.iop.org/JPhysA/41/252001

Abstract

Two new networks are introduced that resemble small-world properties. These networks are recursively constructed but retain a fixed, regular degree. They possess a unique one-dimensional lattice backbone overlaid by a hierarchical sequence of long-distance links, mixing real-space and small-world features. Both networks, one 3-regular and the other 4-regular, lead to distinct behaviors, as revealed by renormalization group studies. The 3-regular network is planar, has a diameter growing as $\sqrt{N}$ with system size N, and leads to super-diffusion with an exact, anomalous exponent $d_w = 1.306\ldots$, but possesses only a trivial fixed point $T_c = 0$ for the Ising ferromagnet. In turn, the 4-regular network is non-planar, has a diameter growing as $\sim 2^{\sqrt{\log_2 N^2}}$, exhibits 'ballistic' diffusion ($d_w = 1$), and a non-trivial ferromagnetic transition, $T_c > 0$. It suggests that the 3-regular network is still quite 'geometric', while the 4-regular network qualifies as a true small world with mean-field properties. As an engineering application we discuss synchronization of processors on these networks.

PACS numbers: 89.75.−k, 64.60.ae, 64.60.aq, 05.50.+q

(Some figures in this article are in colour only in the electronic version)

The description of the '6-degrees-of-separation' phenomenon in terms of small-world (SW) networks by Watts and Strogatz [1] has captured the imagination of many researchers, and was particularly timely as we suddenly found ourselves in a networked world [2–4]. Such a rich environment requires a diverse set of tools and models for their understanding. Statistical physics, with its notion of universality, provides powerful methods for the classification of complex systems, like the renormalization group (RG) [5–8].

Here, we introduce and study a set of graphs which reproduce the behavior of SW networks without the usual disorder inherent in natural networks. Instead, they attain these properties in a recursive, hierarchical manner that is conducive for RG. The motivation is comparable to regular scale-free networks proposed in [9, 10] or the Migdal–Kadanoff RG [11–13]. The benefit of these features is two-fold: for one, we expect that many SW phenomena can be studied analytically on these networks, and that they will prove as useful as, say, Migdal–Kadanoff RG has been for physical systems in low dimensions. Furthermore, possessing such

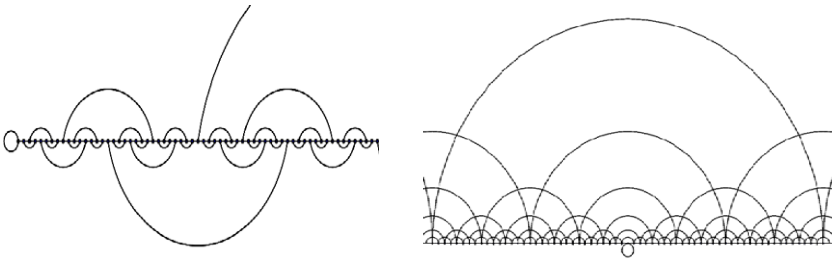

Figure 1. Display of the 3-regular network HN3 (left) and 4-regular network HN4 (right). HN3 is planar but HN4 is not.

well-understood and *regular* networks is a tremendous advantage for engineering applications, as it is difficult to manufacture realizations of *random* networks reliably when we can ascertain their behavior only in the ensemble average. Here, we introduce these networks by discussing their geometry and physical processes on them, such as diffusion, phase transitions and synchronization.

Each network possesses a geometric backbone, a one-dimensional line of $N = 2^k$ sites, either open or closed into a ring. To obtain a SW hierarchy, we parameterize

$$n = 2^i (2j + 1) \tag{1}$$

uniquely for any integer $n \neq 0$, where $j = 0, \pm 1, \pm 2, \ldots$ labels consecutive sites within each level $i \geqslant 0$ of the hierarchy. For instance, $i = 0$ refers to all odd integers, $i = 1$ to all integers once divisible by 2 (i.e., $\pm 2, \pm 6, \pm 10, \ldots$), and so on. In these networks, both depicted in figure 1, in addition to its nearest neighbor in the backbone, each site is also connected with one (or both) of its neighbors *within* the hierarchy. For example, we obtain a hierarchical 3-regular network HN3 by connecting first neighbors in the 1D backbone, then 1–3, 5–7, 9–11, etc, for $i = 0$, next 2–6, 10–14, etc, for $i = 1$, and 4–12, 20–28, etc, for $i = 2$, and so on. The 4-regular network HN4 is obtained in the same manner, but connecting to *both* neighbors in the hierarchy. For HN4 it is clearly preferable to extend the line to $-\infty < n < \infty$ and also connect -1 to 1, -2 to 2, etc, as well as all negative integers in the above pattern. These networks resemble models of ultra-diffusion [14, 15], but with inhibiting barriers replaced by short-cuts here.

It is simple to determine geometric properties. For instance, both networks have a clustering coefficient [2] of $1/4$. Next, we consider the diameter d, the longest of the shortest paths between any two sites, here the end-to-end distance. Using system sizes $N_k = 2^k, k = 2, 4, 6, \ldots$, for HN3, the diameter path looks like a Koch curve, see figure 2. The length d_k of each marked path is given by $d_{k+2} = 2d_k + 1$ for $N_{k+2} = 4N_k$, hence

$$d \sim \sqrt{N}. \tag{2}$$

This property is reminiscent of a square lattice of N sites, whose diameter (=diagonal) is also $\sim\sqrt{N}$. HN3 is thus far from true SW behavior where $d \sim \ln N$.

The geometry of HN4 is more subtle. We consider again the shortest path between the origin $n = 0$ and the end $n = N = 2^k$. Due to degeneracies at each level, one has to probe many levels in the hierarchy to discern a pattern. In fact, any pattern evolves for an increasing number of levels before it gets taken over by a new one, with two patterns creating degeneracies at the crossover. We find that the paths here do *not* search out the longest possible jump, as in figure 2. Instead, the paths reach quickly to some intermediate level and follow *consecutive* jumps at that level before trailing off in the end. This is a key distinguishing feature between

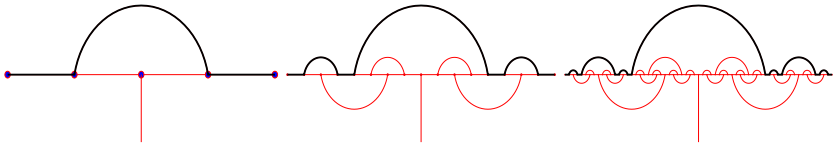

Figure 2. Sequence of shortest end-to-end paths (=diameter, thick lines) for HN3 of size $N = 2^k, k = 2, 4, 8$. Whenever the system size N increases by a factor of 4, the diameter d increases by a factor of ∼2, leading to equation (2).

HN3 and HN4: once a level is reached in HN4, the entire network can be traversed at that level, while in HN3 one *must* switch to lower levels to progress, see figure 1.

We derive a recursion equation [16] with the solution

$$d \sim \tfrac{1}{2}\sqrt{\log_2 N^2}\, 2^{\sqrt{\log_2 N^2}} \quad (N \to \infty) \tag{3}$$

for the diameter of HN4. Expecting the diameter of a small world to scale as $d \sim \log N$, we rewrite equation (3):

$$d_k \sim (\log_2 N)^{\alpha} \qquad \text{with} \qquad \alpha \sim \frac{\sqrt{\log_2 N^2}}{\log_2 \log_2 N} + \frac{1}{2}. \tag{4}$$

Technically, α diverges with N and the diameter grows faster than any power of $\log_2 N$ (but less than any power of N, unlike equation (2)). In reality, though, α varies only very slowly with N, ranging merely from $\alpha \approx 1.44$ to ≈1.84 over *nine* orders of magnitude, $N = 10$–10^{10}.

As a demonstration of the rich dynamics facilitated by these networks, we have modeled diffusion on HN3 and HN4. Starting a random walk at $n = 0$, we focus here only on the mean displacement with time,

$$\langle |n| \rangle \sim t^{1/d_w}. \tag{5}$$

All walks are controlled by the probability p of a walker to step off the lattice into the direction of a long-range jump. In particular, the walker always jumps either to the left or right neighbor with probability $(1 - p)/2$, but makes a long-range jump with probability p on HN3, or $p/2$ to either the left or right on HN4. In both cases, a simple 1D nearest-neighbor walk results for $p = 0$ with $d_w = 2$ for ordinary diffusion. For any probability $p > 0$, long-range links will dominate the asymptotic behavior, and the leading scaling behavior becomes independent of p.

Adapting the RG for random walks in [17, 18], we find *exact* results for HN3. The local analysis[19] of the physical fixed point is *singular*, with a boundary layer instead of a Taylor expansion, yielding an anomalous exponent of $d_w = 2 - \log_2(\phi) = 1.3057581\ldots$, containing the (irrational) 'golden section' $\phi = (1 + \sqrt{5})/2$. This is a remarkable exponent also because it is a rare example of a simple walk with super-diffusive ($1 < d_w < 2$) behavior without Levy flights [20–22], and it would be consistent with experiments leading to super-diffusion [23]. We have not been able to extend this RG calculation to obtain analytic results for HN4 yet, although the high degree of symmetry inherent in these networks (and the simple result obtained) suggests the possibility. For HN4, an annealed approximation and simulations, evolving some 2×10^7 walks for 10^6 time steps each, suggest a value of $d_w = 1$, see figure 3. Hence, a walk on HN4 proceeds effectively ballistic, but hardly with linear motion: widely fluctuating jumps conspire just so that a single walker extends outward with an on-average constant velocity in *both* directions, yet the walk remains recurrent. Clearly, it is easier to traverse HN4 than HN3 because of the above-stated fact that on HN4 a walker can progress *repeatedly* within a hierarchical level.

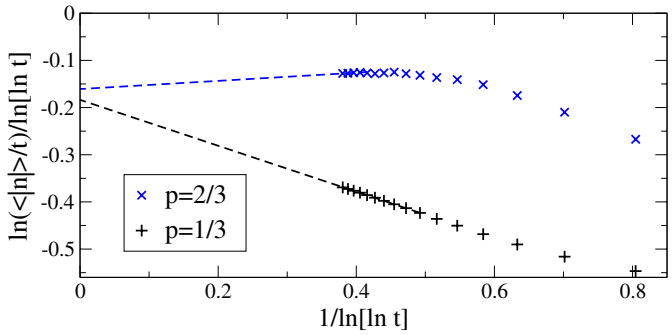

Figure 3. Rescaled plot of the mean distance $\langle|n|\rangle$ in HN4 for walks up to $t = 10^6$. We demonstrate that $d_w = 1$ but with log corrections by rewriting equation (5) as $\langle|n|\rangle/t \sim V[\ln t]^{\beta}$. Then we obtain $\ln(\langle|n|\rangle/t)/\ln[\ln t] \sim \beta + \ln V/\ln[\ln t]$ and linearly extrapolate (dashed lines) $1/\ln[\ln t] \to 0$, estimating $\beta \approx -0.18$ at the intercept, independent of p. An effective 'velocity' V could be extracted from the slope. For any value besides $d_w = 1$, these extrapolations would *not* converge.

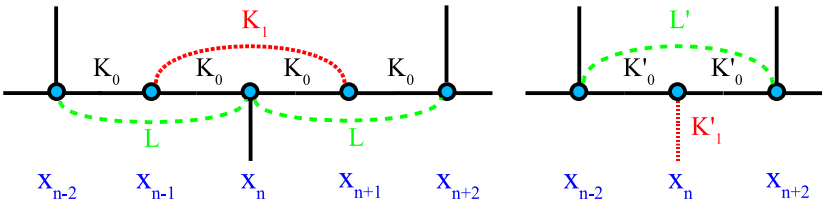

Figure 4. Depiction of (exact) RG step for the Ising model on HN3. Tracing out odd-labeled variables $x_{n\pm1}$ for all $n = 2(2j+1)$, in the left plot leads to the renormalized couplings (L', K_0', K_1') on the right in terms of the old couplings (L, K_0, K_1). Unlabeled bonds correspond to $K_{i\geqslant 2}$. HN3 does not contain couplings of type (L, L'), but they become relevant during the RG process. Random walks on HN3 lead to a topologically equivalent, but more involved RG step [19].

We have also studied Ising spin models on HN3 and HN4, with RG and with Monte Carlo simulations. First, we consider the RG for the Ising model on HN3. In this case, all steps can be done exactly but the result turns out to be trivial (for uniform bonds) in the sense that there are no finite-temperature fixed points of the RG flow. Yet, the calculation is instructive, highlighting the large number of statistical models that can be accessed through the hierarchical nature of the process, and it is *almost* identical in outcome to the treatment below for HN4. That small difference is just enough to provide HN4 with a non-trivial $T_c > 0$, which we confirm numerically.

The RG consists of recursively tracing out odd-relabeled spins $x_{n\pm1}$, see figure 4. $x_{n\pm1}$ are connected to their even-labeled nearest neighbors on the lattice backbone by a coupling K_0. At any level, each $x_{n\pm1}$ is also connected to another such spin $x_{n\mp1}$ across an even-labeled spin x_n with $n = 2(2j+1)$ in equation (1) that is exactly *once* divisible by 2. Let us call that coupling K_1, all other couplings are $K_{i>1}$. During the RG process, a new coupling L (dashed line in figure 4) between next-nearest even-labeled neighbors emerges. Putting all higher level terms into $\mathcal{R}$, we can section the Hamiltonian

$$-\beta\mathcal{H} = \sum_{\{n=2(2j+1)\}} (-\beta\mathcal{H}_n) + \mathcal{R}(K_2, K_3, \ldots), \tag{6}$$

where each sectional Hamiltonian is given by

$$-\beta\mathcal{H}_n = \sum_{m=n-2}^{n+1} K_0 x_m x_{m+1} + K_1 x_{n-1} x_{n+1} + L(x_{n-2}x_n + x_n x_{n+2}) \tag{7}$$

with (K_0, K_1, L) as unrenormalized couplings and we neglected an overall energy scale L. After tracing out the odd-labeled spins in each $\exp[-\beta\mathcal{H}_n]$, we identify the renormalized couplings (neglecting I'):

$$\begin{aligned} K_0' &= L + \tfrac{1}{2}\ln\cosh(2K_0) + \tfrac{1}{4}\ln[1+\tanh(K_1)\tanh^2(2K_0)], \\ L' &= \tfrac{1}{4}\ln[1+\tanh(K_1)\tanh^2(2K_0)], \end{aligned} \tag{8}$$

and $K_i' = K_{i+1}$ f. a. $i \geqslant 1$. The high-T solution $K_0^* = L^* = 0$ is a trivial fixed point of equation (8). Excluding that and eliminating L^* yields $1 = \tanh(K_1)\tanh\left(2K_0^*\right)$, which has only the $T_c = 0$ solution $K_0^* = \infty$ (where also $K_1 = J_1/T \to \infty$). Note, however, that the RG recursions (8) have a remarkable property due to the hierarchical structure of the network: the next-level coupling K_1 appears as a *free parameter* and acts as 'source term' that could be chosen to represent physically interesting situations, e.g. disorder or distance dependence. For instance, with K_i as an increasing function of distance $r_i = 2^{i+1}$, a non-trivial fixed point could be created.

In contrast, HN4 provides a non-trivial solution for the Ising model even for uniform bonds, as expected for a mean-field system. Again, an exact result for HN4 is elusive, although in light of the inherent symmetries such a solution appears possible. Instead, we proceed to a Niemeijer–van Leeuwen cumulant expansion [7] and compare with our numerical simulations. The Hamiltonian indeed has an elegant hierarchical form separating the lattice backbone and long-range couplings:

$$-\beta\mathcal{H} = \sum_{n=1}^{2^k} K_0 x_{n-1} x_n + \sum_{i=1}^{k}\sum_{j=1}^{2^{k-i}} K_i x_{2^{i-1}(2j-1)} x_{2^{i-1}(2j+1)}. \tag{9}$$

For the RG, we set $-\beta\mathcal{H} = -\beta\mathcal{H}_0 - \beta\mathcal{V} + \mathcal{R}$ with

$$-\beta\mathcal{H}_0 = \sum_{j=1}^{2^{k-1}} K_0 x_{2j-1}(x_{2j-2} + x_{2j}) + \sum_{j=1}^{2^{k-1}} L x_{2j-2} x_{2j}, \qquad -\beta\mathcal{V} = \sum_{j=1}^{2^{k-1}} K_1 x_{2j-1} x_{2j+1}, \tag{10}$$

adding new couplings L that emerge during RG, as in figure 4. Tracing out odd spins and relabeling all remaining even spin variables $x_n \to x'_{n/2}$, the cumulant expansion applied to equation (10) yields a new Hamiltonian $-\beta\mathcal{H}'$, formally *identical* to equation (9), with the rescaled couplings

$$\begin{aligned} K_0' &= L + \frac{1}{2}\ln\cosh(2K_0) + \frac{K_1}{2}\tanh^2(2K_0), \\ K_1' &= K_2 + \frac{K_1}{4}\tanh^2(2K_0), \qquad L' = \frac{K_1}{4}\tanh^2(2K_0). \end{aligned} \tag{11}$$

and $K_i' = K_{i+1}$ for $(i \geqslant 2)$. These are the same relation one would obtain for the 1D Ising model with *nnn* couplings, if $K_1 \equiv L$ and $K_i = 0$ for $i \geqslant 2$. In that case, one would find—correctly—that there are *no* non-trivial fixed points. The K_2 term, which appears as an arbitrary source again at every RG step, if chosen appropriately, provides the sole ingredient for a non-trivial outcome. But unlike for HN3, here already uniform (i-independent) K_i obtain $T_c > 0$. Holding the source terms fixed, $K_{i\geqslant 2} \equiv 1$, we find a single nontrivial fixed point at $K_0^* \approx 0.2781$, $K_1^* \approx 1.0681$, $L^* \approx 0.0681$. An analysis of the RG flow [7] in equations (11), starting with identical $K_i \equiv \beta J$ f. a. i, yields $T_c \approx 2.2545J$. Simulations

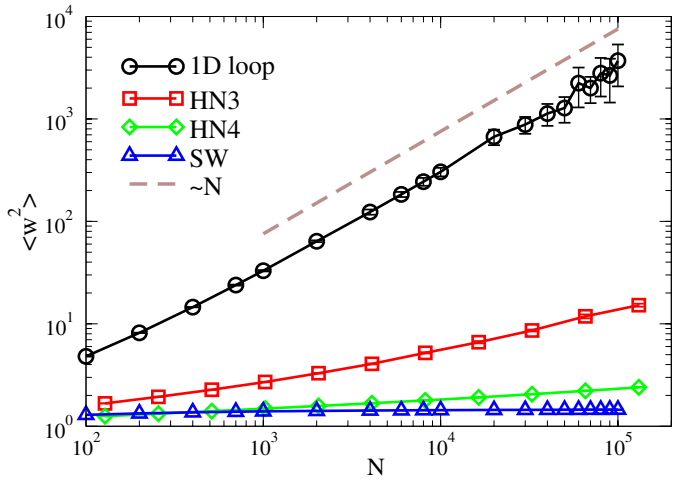

Figure 5. Width $< w^2 >$ as a function of N. The 1D loop without long-range connections diverges most strongly, linear in N, while the random one-per-node SW connections keep the width finite. The width diverges with a weak power of N for HN3, but merely logarithmically for HN4.

on HN4 with uniform bonds for increasing system sizes $N = 2^k$ accumulate to $T_c = 2.1(1)J$.

Finally, we demonstrate the usefulness of having a regular (i.e., non-random) network at hand with fixed, *predictable* properties. Synchronization is a fundamental problem in natural and artificially coupled multicomponent systems [24]. Since the introduction of SW networks [1], it has been established that such networks can facilitate autonomous synchronization [25, 26]. In a particular synchronization problem the nodes are assumed to be task processing units, such as computers or manufacturing devices. Let $h_i(t)$ be the total task completed by node i at time t and the set $\{h_i(t)\}_{i=1}^N$ constitutes the task-completion (synchronization) landscape, where N is the number of nodes. In this model the nodes whose tasks are smaller than those of their neighbors are incremented by an exponentially distributed random amount, i.e., the node i is incremented, if $h_i(t) \leqslant \min_{j\in S_i}\{h_j(t)\}$, where S_i is the set of nodes connected to node i; otherwise, it idles. In its simplest form the evolution equation is $h_i(t+1) = h_i(t) + \eta_i(t) \prod_{j\in S_i} \Theta(h_j(t) - h_i(t))$, with *iid* random variables of unit mean, $\eta_i(t)$, δ correlated in space and time and Θ as the Heaviside step function.

The average steady-state spread or width of the synchronization landscape (degree of de-synchronization) can be written as $w^2 = (1/N)\sum_{i=1}^N (h_i - \bar{h})^2$ [26]. In low-dimensional regular lattices the synchronization landscape belongs to the Kardar–Parisi–Zhang [27] universality class, a rough desynchronized state dominated by large-amplitude long-wavelength fluctuations, where width diverges with N. In contrast, the width becomes finite [26] on a SW model in which each node is connected to nearest neighbors and one random neighbor. In figure 5, we show the width as a function of N for a 1D loop and SW, as well as HN3 and HN4. The width for HN4 behaves very similar to SW, with at most a logarithmic divergence in N, while it diverges with power law for HN3, but weaker than for a 1D loop. HN4, thus, provides very similar properties to SW with the benefit of a regular and reproducible structure that is easy to manufacture, and that is potentially analytically tractable.

In conclusion, we introduced a new set of hierarchical networks with regular, small-world properties and demonstrated their usefulness for theory and engineering applications with a

few examples. Aside from the countless number of statistical models that can be explored with RG on these networks, they also provide a systematic way to interpolate off a purely geometric lattice into the SW domain, possibly all the way into the mean-field regime (for HN4). Even though at this point complete solutions on HN4 elude the authors, even the leading approximation provides significant insight.

Acknowledgments

BG was supported by the NSF through grant #0312510 and HG was supported by the US DOE through DEAC52-06NA25396.

References

[1] Watts D J and Strogatz S H 1998 Collective dynamics of 'small-world' networks *Nature* **393** 440–2
[2] Boccaletti S, Latora V, Moreno Y, Chavez M and Hwang D-U 2006 Complex networks: structure and dynamics *Phys. Rep.* **424** 175
[3] Barabasi A-L 2003 *Linked: How Everything Is Connected to Everything Else and What It Means for Business, Science, and Everyday Life* (Cambridge: Perseus Books)
[4] Newman M E J, Strogatz S H and Watts D J 2001 Random graphs with arbitrary degree distributions and their applications *Phys. Rev.* E **64** 026118
[5] Goldenfeld N 1992 *Lectures on Phase Transitions and the Renormalization Group* (Reading, MA: Addison-Wesley)
[6] Stanley H E 1999 Scaling, universality, and renormalization: three pillars of modern critical phenomena *Rev. Mod. Phys.* **71** S358–66
[7] Plischke M and Bergersen B 1994 *Equilibrium Statistical Physics* 2nd edn (Singapore: World Scientifc)
[8] Newman M E J and Watts D J 1999 Renormalization group analysis of the small-world network model *Phys. Lett.* A **263** 341–6
[9] Barabasi A-L, Ravasz E and Vicsek T 2001 Deterministic scale-free networks *Physica* A **299** 559–64
[10] Andrade J S, Herrmann H-J, Andrade R F S and da Silva L R 2005 Apollonian networks: simultaneously scale-free, small world, Euclidean, space filling, and with matching graphs *Phys. Rev. Lett.* **94** 018702
[11] Migdal A A 1976 *J. Exp. Theor. Phys.* **42** 743–6
[12] Kadanoff L P 1976 *Ann. Phys.* **100** 359–94
[13] Hinczewski M and Berker A N 2006 Inverted Berezinskii–Kosterlitz–Thouless singularity and high-temperature algebraic order in an Ising model on a scale-free hierarchical-lattice small-world network *Phys. Rev.* E **73** 066126
[14] Huberman B A and Kerszberg M 1985 Ultradiffusion: the relaxation of hierarchical systems *J. Phys. A: Math. Gen.* **18** L331–6
[15] Ogielski A T and Stein D L 1985 Dynamics on ultrametric spaces *Phys. Rev. Lett.* **55** 1634–7
[16] Boettcher S, Gonçalves B and Azaret J 2008 Geometry and dynamics for hierarchical regular networks *Preprint* arXiv:0805.3013
[17] Kahng B and Redner S 1989 Scaling of the first-passage time and the survival probability on exact and quasi-exact self-similar structures *J. Phys. A: Math. Gen.* **22** 887–902
[18] Redner S 2001 *A Guide to First-Passage Processes* (Cambridge: Cambridge University Press)
[19] Boettcher S and Gonçalves B 2008 Anomalous diffusion on the Hanoi network *Preprint* 0802.2757
[20] Havlin S and Ben-Avraham D 1987 Diffusion in disordered media *Adv. Phys.* **36** 695–798
[21] Metzler R and Klafter J 2004 The restaurant at the end of the random walk: recent developments in the description of anomalous transport by fractional dynamics *J. Phys. A: Math. Gen.* **37** R161–208
[22] Fischer A, Seeger S, Hoffmann K-H, Essex C and Davison M 2007 Modeling anomalous superdiffusion *J. Phys. A: Math. Theor.* **40** 11441–52
[23] Solomon T H, Weeks E R and Swinney H L 1993 Observation of anomalous diffusion and lévy flights in a two-dimensional rotating flow *Phys. Rev. Lett.* **71** 3975–8
[24] Strogatz S 2001 *Nature* **410** 268
[25] Barahona M and Pecora L M 2002 Synchronization in small-world systems *Phys. Rev. Lett.* **89** 054101
[26] Korniss G, Novotny M A, Guclu H, Toroczkai Z and Rikvold P A 2003 Suppressing roughness of virtual times in parallel discrete-event simulations *Science* **299** 677–9
[27] Kardar M, Parisi G and Zhang Y-C 1986 *Phys. Rev. Lett.* **56** 889